FRET-Paired Hydrogel Forming Silk-Elastin-Like Recombinamers by Recombinant Conjugation of Fluorescent Proteins

Arturo Ibáñez-Fonseca, Matilde Alonso, Francisco Javier Arias, José Carlos Rodríguez-Cabello*

BIOFORGE Lab, University of Valladolid – CIBER-BBN, Paseo de Belén 19, 47011 – Valladolid, Spain

Corresponding author:

* Prof. J.C. Rodríguez-Cabello. Paseo de Belén, 19, 47011 – Valladolid (SPAIN). E-mail: roca@bioforge.uva.es. Phone: +34983184585.

Abstract

In the last decades, recombinant structural proteins have become very promising in addressing different issues like the lack of traceability of biomedical devices or the design of more sensitive biosensors. Among them, we find elastin-like recombinamers (ELRs), which can be designed to self-assemble into diverse structures, like hydrogels. Furthermore, they might be combined with other protein polymers, such as silk, to give silk-elastin-like recombinamers (SELRs), holding the properties of both proteins. In this work, due to their recombinant nature, we have fused two different fluorescent proteins (FPs), i.e. the green *Aequorea coerulescens* EGFP and the near-infrared eqFP650, to a SELR able to form irreversible hydrogels through physical cross-linking. These recombinamers showed an emission of fluorescence similar to the single FPs, and they were capable of forming hydrogels with different stiffness (G' = 60-4000 Pa), by varying the concentration of the SELR-FPs. Moreover, the absorption spectrum of SELR-eqFP650 showed a peak greatly overlapping the emission spectrum of the SELR-

AcEGFP, hence enabling Förster resonance energy transfer (FRET) upon the interaction between two SELR molecules, each one containing a different FP, due to the stacking of silk domains at any temperature and to the aggregation of elastin-like blocks above the transition temperature. This effect was studied by different methods and a FRET efficiency of 0.06-0.2 was observed, depending on the technique used for its calculation. Therefore, innovative biological applications arise from the combination of SELRs with FPs, such as enhancing the traceability of hydrogels based on SELRs intended for tissue engineering, the development of biosensors, and the prediction of FRET efficiencies of novel FRET pairs.

Introduction

The combination of peptides and proteins holding specific properties with other molecules may lead to the engineering of novel materials with improved features that can be exploited in different biological applications. This can be achieved through the chemical conjugation of (poly)peptides to other molecules able to form diverse types of structures.[1] However, recombinant protein-based materials are much more interesting in terms of conjugation to other proteins, since the fusion protein can be obtained by genetic engineering methods and further expression in a heterologous host.[2]

Regarding specific recombinant polymers, elastin-like recombinamers (ELRs), a terminology that highlights the recombinant nature of elastin-like polypeptides first described by Urry *et al.*,[3] have been extensively used for the development of different materials in the recent years.[4-6] ELRs comprise repetitive units of the Val-Pro-Gly-X-Gly $(VPGXG)_n$ pentapeptide in which X (guest residue) is any amino acid except L-proline. Moreover, they show thermosensitivity due to the change of the protein conformation above the so-called transition temperature (T_t), which itself depends on

the polarity of the side chain in the guest residue.[7] Therefore, the T_t can be tuned depending on the amino acid chosen in the X position of the pentapeptide.[8,9] Furthermore, ELRs can be designed so the phase transition occurring above the T_t is translated into a hydrophobically-driven self-assembly of the molecules towards supramolecular structures such as particles,[10] micelles and vesicles,[11] electrospun fibers[12] and hydrogels,[13] among others. In addition, ELRs can be fused to repeated amino acid sequences derived from other structural proteins like the GAGAGS hexapeptide found in *Bombyx mori* silk fibroin, hence giving rise to silk-elastin-like recombinamers (SELR),[14] to form more complicated structures, e.g. hydrogels, that incorporate the properties of both polypeptides.[15]

In this work, we have fused two different fluorescent proteins (FPs) to a previously described amphiphilic SELR[15] based on two types of elastin-like domains, one hydrophilic and the other one hydrophobic, by including glutamic acid and isoleucine as guest residues, respectively. This SELR is able to self-assemble into hydrogels that are injectable below the T_t, through the transition mechanism due to the hydrophobic ELR blocks, while the formed network is further stabilized by the silk domains. First, we have fused a green-emitting FP to the SELR used in this study, namely *Aequorea coerulescens* enhanced green fluorescent protein (AcEGFP).[16,17] In another molecule maintaining the same SELR structure, we have cloned the near-infrared-emitting eqFP650, which was previously described as the brightest FP above 635 nm.[18] Furthermore, this protein was shown to behave as a dimer, which could be a disadvantage in the case of fusion proteins, since it may hamper dimerization and efficient emission of fluorescence. However, we intended to assess if this kind of oligomeric FPs kept their fluorescence when used to improve the properties of protein-based materials, such as ELRs or SELRs. For instance, there exist many dimeric and

tetrameric far-red and infrared FPs that are very useful in *in vivo* applications as they avoid the drawbacks that arise from the use of GFP, YFP or orange FPs, like a low signal-to-noise ratio due to the excitation and emission of auto-fluorescence by endogenous molecules, such as hemoglobin, at the wavelength ranges of these FPs.[19] Both fluorescent SELRs (SELR-FPs) were characterized by physicochemical methods and the mechanical properties of the hydrogels based on these recombinamers were also evaluated.

Moreover, with the aim of exploring novel approaches beyond simple fluorescence emission, we studied Förster resonance energy transfer (FRET).[20] High FRET efficiencies are achieved when the distance between the donor and the acceptor is in the range of 1-10 nm, they have a favourable dipole-dipole alignment, and there is a significant spectral overlap of the donor emission and acceptor excitation (or absorption) spectra.[21] Hence, the study of FRET between both SELR-FPs by spectroscopy (donor quenching) and confocal microscopy (acceptor photobleaching) allowed us to get information about the interaction between SELR molecules varying from low to high concentration solutions, at which they self-assemble into particles and hydrogels, respectively, as described for the SELR itself.[15] Although a previous work described a FRET effect between ELR molecules fused to fluorescent proteins, this was only feasible if other polypeptides forming a specific protein complex were included in the final protein.[22] In our case, our hypothesis relies on the ability of SELR molecules of establishing stacking interactions at mid and high concentrations that are able to minimize the distance between the two FPs, hence enabling FRET. Moreover, the formation of SELR-FPs-based hydrogels increases the potential of this FRET system in different applications. In addition, this is the first time that FRET is described for this pair of FPs, to our best knowledge.

This work aimed to show the development of novel fluorescent SELRs and the study of the features inherent to the SELR, to the FPs and to their combination. The results described below provide the basis for further studies regarding the potential applications of the hydrogel-forming SELR-FPs designed and bioproduced in this work as biosensors,[23] taking advantage of their recombinant nature. Thereby, peptides/proteins that bind to different targets may be included in the SELR sequence, such as glucose,[24] LPS,[25] or metal ions,[26] thus showing an enormous potential in the field of biosensors. Furthermore, the use of FRET could considerably increase the sensitivity of these SELR-based biosensors due to the measurement through ratiometric instead of intensiometric measurements.[27] Likewise, SELR-FPs might be used to enhance the traceability of biomedical devices made of themselves or in combination with other ELRs or silk-based materials.

Results and Discussion

Fluorescent SELRs design, bioproduction and physicochemical characterization

The genes of the SELRs designed for the purpose of this work were successfully synthetized (see Figure S1 for a schematic representation of both SELR-FPs and Table S1 for the full abbreviated amino acid sequence) and all the cloning steps were carefully evaluated by agarose gel electrophoresis and DNA sequencing methods (data not shown). Further expression of SELRs in *E. coli* was confirmed by SDS-PAGE, and a final yield of 133 and 120 mg/L of lyophilized product was obtained for the SELR-AcEGFP and the SELR-eqFP650, respectively. These results are lower than the one found previously for the SELR itself,[15] hence indicating that the fusion of both FPs hinders the expression and/or the purification of the SELR.

The purity and molecular weight (*Mw*) of the final products were assessed by SDS-PAGE and MALDI-TOF (Figure S2 and Figure S3, respectively). As regards the purity, it was found to be ≥ 95% for both recombinamers. In the case of the *Mw*, the experimental values, obtained from the m/2z value, (126.9 and 128.9 kDa for SELR-AcEGFP and SELR-eqFP650, respectively) were very similar to the expected values (128.7 and 128.1 kDa) for both SELR-FPs. Additional characterization included H-NMR spectroscopy (Figure S4 and Tables S6 and S7) and amino acid composition by HPLC (Table S2 and S3 for SELR-AcEGFP and SELR-eqFP650, respectively), confirming the absence of undesired contaminants. Furthermore, the transition process was studied by DSC and SELR-AcEGFP and SELR-eqFP650 showed a T_t of 16.8 and 17.2ºC, respectively, in PBS at neutral pH (Figure S5). This temperature is more than 2ºC higher than the one found for the SELR alone (14.4ºC),[15] since the hydrophilic FPs fused to this recombinamer increase the overall hydrophilicity of the final protein, and therefore the T_t raises, in agreement with a previous work by Chilkoti and co-workers.[28] Moreover, DSC results show that both SELR-FPs meet the requirements to be used in biomedical applications, since the transition of the recombinamers at body temperature (37ºC) will give rise to hydrogels at high concentrations of the SELR-FPs, as shown below.

Mechanical properties of hydrogels based on SELR-FPs

The formation of SELR hydrogels is described in depth by Fernández-Colino *et al.*[15] Briefly, hydrophobic interactions between elastin-like blocks initiate the formation of the hydrogel network once the temperature is raised above the T_t. This brings silk-like domains together, allowing the hydrogen bonding between them in a process termed "annealing", which leads to an increase of the stiffness and to a complete stabilization of the hydrogels over time.

As observed in Figure 1, both SELR-FPs show a decrease in the storage modulus (*G'*) in comparison to the SELR alone at the same molar concentration.[15] For instance, *G'* for SELR-based hydrogels at 1.13 mM are 2.6-, 2.3- and 2.4-fold higher compared to SELR-AcEGFP, SELR-eqFP650 and the 1:1 molar mixture, respectively. On the other hand, the increase at 1.73 mM is 1.3- and 1.4-fold for SELR-AcEGFP and for both SELR-eqFP650 and the 1:1 molar mixture, respectively (see Table S4). These results can be explained by the steric effect due to the high volume occupied by either AcEGFP or eqFP650 that impedes the tight stacking of elastin-like blocks above the T_t and the formation of hydrogen bonds between silk domains that stiffen the hydrogels. However, this effect is counteracted by increasing the concentration of SELR-FPs solutions to form the hydrogels. The differences between SELR-AcEGFP and SELR-eqFP650 are very slight, being more noticeable at higher concentrations (1.94 mM), i.e. *G'* of 4055 and 3354 Pa, respectively. This might be due to the higher steric effect in the case of the eqFP650 (and the 1:1 molar mixture) because this FP tends to form dimers.

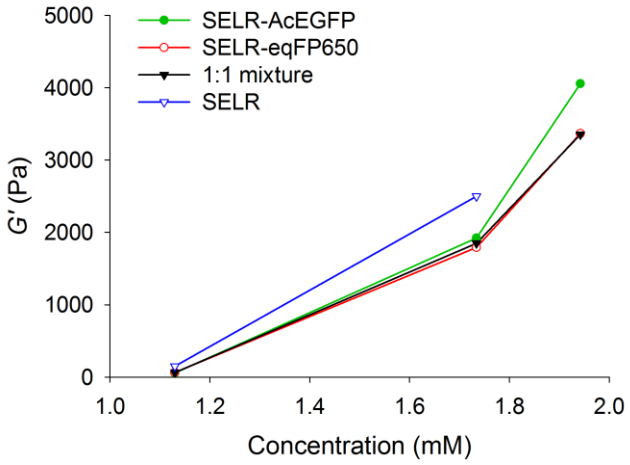

Figure 1. Graph showing the mechanical properties of SELR-FPs-based hydrogels compared to SELR-based ones, in terms of storage modulus (*G'*) at three different concentrations (1.13, 1.73 and 1.94 mM). Data corresponding to SELR only was obtained from Fernández-Colino *et al.*[15]

In addition, results show that it is possible to obtain hydrogels with different grades of stiffness depending on the concentration, hence being suitable for diverse applications in tissue engineering.[29] For example, very soft hydrogels with a *G'* of ~60 Pa were achieved at 1.13 mM, while at 1.94 mM (250 mg/mL) a *G'* of ~3700 Pa is observed. Below 145 mg/mL, hydrogels were not formed above the T_t as confirmed by visual evaluation through the inversion of tubes containing the SELR-FPs solutions at this concentration.

Fluorescence characterization of SELR-FPs by spectroscopy

The extinction coefficient (ε) of both SELR-FPs was calculated as stated in the experimental section, following Equation 1. The absorbance (A) was obtained from the absorption spectra at the wavelength of its maximum (λ_{max}), i.e. A = 0.548 for SELR-AcEGFP at 488 nm, while A = 0.800 for SELR-eqFP650 at 589 nm (peak 2 in absorption spectrum, Figure S6). With these values, we calculated ε (see Table 1) and it was found to be 21.7% and 15.8% of the corresponding non-fused FPs, for SELR-AcEGFP and SELR-eqFP650, respectively. We describe two excitation and emission maxima for SELR-eqFP650 due to the two peaks observed in its absorption spectrum (Figure S6), as described below. Hence, in Table 1, excitation peaks 1 and 2 are correlated to emission peaks 1 and 2, respectively.

Table 1. Key properties of SELR-FPs compared to the corresponding single FPs.

properties	AcGFP1 (Clontech)	SELR-AcEGFP	eqFP650 (TurboFP650, Evrogen)	SELR-eqFP650
Excitation peak (nm)	475	475	592	Peak 1 – 516 Peak 2 – 587
Emission peak	505	510	650	Peak 1 – 540

(nm)				Peak 2 – 636
Molar extinction coefficient (ε, M^{-1} cm^{-1}) at excitation maximum	32,500	7,046	65,000	10,243
Fluorescence quantum yield (QY)	0.82	0.34	0.24	0.10
Brightness[a] (a.u.)	26,650	2,396	15,600	1,024
Brightness related to AcGFP1	1	0.09	0.59	0.04
Reference	Commercial brochure	This work	18	This work

[a] Calculated as the product of ε and QY.

Furthermore, the brightness, as calculated here, taking other works as references, is very low compared to SELR-FPs counterparts. However, it should be noticed that a great amount of molecules is present in a SELR-FP-based hydrogel, so it will be clearly visible by *in vivo* imaging systems or other instruments dedicated to detect fluorescence.

Moreover, the excitation and emission spectra of both SELR-FPs (Figure 2) were in good agreement with those found in the literature for AcGFP and other derivatives,[16,17] and for eqFP650.[18] Nevertheless, in the latter case, excitation and emission λ_{max} were found slightly shifted for SELR-eqFP650, meaning that the fusion to SELR may impede correct maturation or dimerization of the FP, hence changing chromophore conformation and, consequently, excitation and emission behavior.

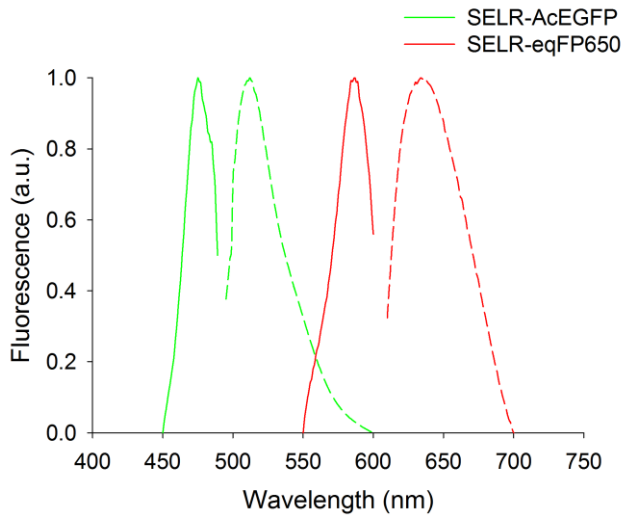

Figure 2. Excitation and emission spectra for SELR-AcEGFP (green solid and dotted lines) and SELR-eqFP650 (red solid and dotted lines).

However, although not observed in the excitation spectrum of SELR-eqFP650 in Figure 2 due to the settings used for its calculation, we observed a peak at 521 nm in the absorbance spectrum of SELR-eqFP650 (Figure S6). The appearance of this peak might be due to an incomplete dimerization or incorrect folding of the far-red FP, which would be hindered by the high molecular weight of the SELR fused to it. This peak presents a high overlap with the one found in the emission spectrum of SELR-AcEGFP (see Figure 3 for a more clear comparison). Therefore, we hypothesized that it may exist a FRET effect between both SELR-FPs, and different studies were performed in this regard, as shown below.

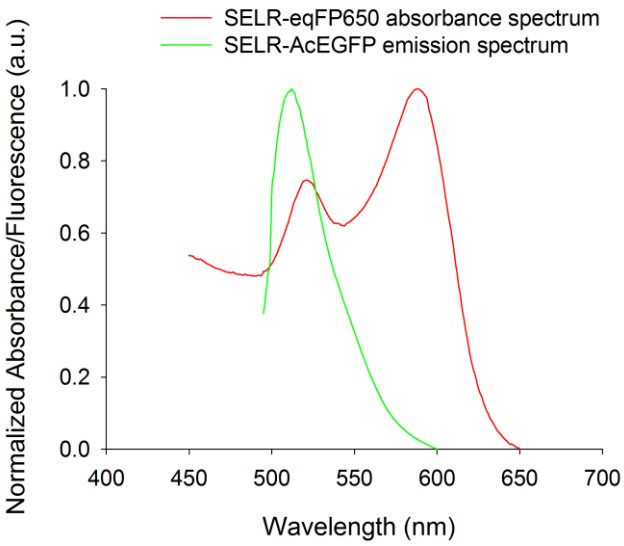

Figure 3. Overlay of the absorbance spectrum of SELR-eqFP650 and the emission spectrum of SELR-AcEGFP showing the high overlap occurring between them.

Calculation of FRET efficiency in SELR-FPs mixtures by spectroscopy (donor quenching)

The experimental determination of the FRET efficiency (*E*) by spectroscopy was achieved through the comparison of the fluorescence intensity emitted by SELR-AcEGFP in the presence and in the absence of SELR-eqFP650. It is widely described that quenching on the fluorescence emitted by the donor of a FRET pair occurs in the presence of the acceptor.[20] In order to obtain *E* accurately, we prepared samples containing the same amount of SELR-FPs, separately, than the quantity used to prepare the 1:1 molar mixture. First, spectra were obtained above T_t setting λ_{ex} at 475 nm, i.e. SELR-AcEGFP maximum, at different concentrations. Then, data from SELR-eqFP650 were subtracted from the ones of the mixture and a direct comparison was performed by representing spectra from SELR-AcEGFP only and from the mixture, as it can be seen in Figure 4.

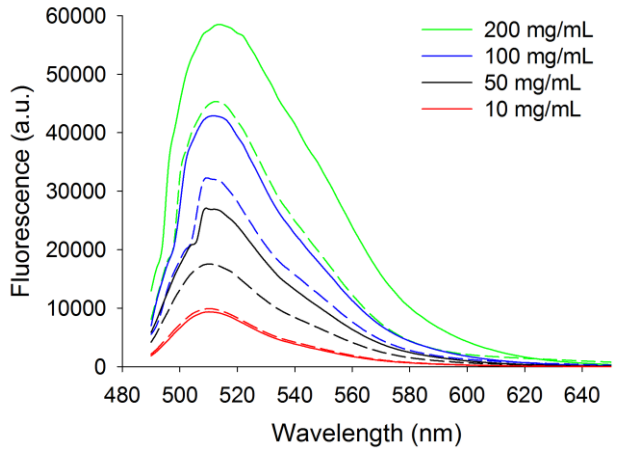

Figure 4. Emission spectra (λ_{ex} = 475 nm) of SELR-AcEGFP (solid lines) and of a 1:1 molar mixture (dotted lines) of both SELR-FPs at different concentrations.

It can be observed that fluorescence intensity is clearly reduced in the case of the mixture (dotted lines) when compared to the SELR-AcEGFP only (solid lines) for every concentration excepting 10 mg/mL, which was the lowest concentration tested. This result indicates that a FRET effect, by means of donor quenching, takes place at mid and high concentrations, probably due to the increased proximity (1-10 nm) between the FPs conjugated to the SELRs.

Concerning *E* values obtained by this technique, we studied the FRET behavior of SELR-FPs at two different temperatures, namely 15 and 37ºC, which are below and above the T_t, respectively. The results (Figure 5) show that FRET is non-existent for the 1:1 molar mixture at 10 mg/mL, as expected by the observation of spectra in Figure 4. Furthermore, there are not significant differences between the FRET efficiencies obtained for the different concentrations and temperatures ($p > 0.05$), excepting between 10 mg/mL and the rest of concentrations. The exact values of *E* obtained for each sample are shown in Table S5.

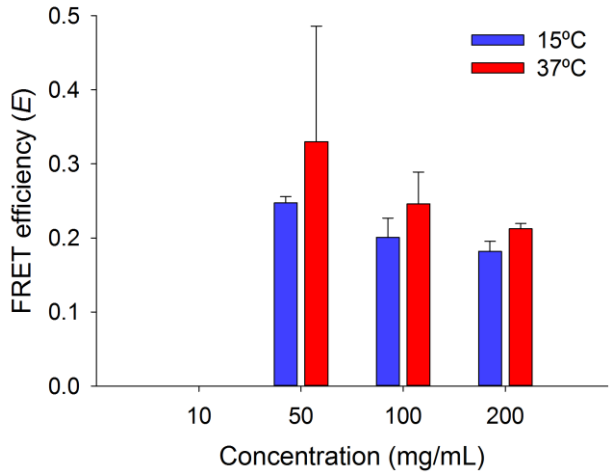

Figure 5. FRET efficiencies calculated by spectroscopy (donor quenching) below (15ºC, blue bars) and above (37ºC, red bars) the T_t, at different concentrations. Data are represented as mean ± SD (n = 2).

The lack of dissimilarities between the different conditions tested suggests that once a minimum concentration is reached, the distance between SELR-FPs molecules is low enough to enable FRET (1-10 nm), independently of the aggregation of the elastin-like blocks above the T_t. Nevertheless, silk-like domains are able to establish interactions between them at any temperature and may help molecules to stack and remain closer even at temperatures below the T_t. Moreover, even though p-values do not indicate significant differences, it can be observed an increase in E above T_t because of the hydrophobic interaction of the elastin-like blocks included in the SELR-FPs.

The evaluation of E in further combinations of elastin- and silk-like domains, and FPs, e.g. including both FPs in the same molecule, may shed light into the structure of particles and hydrogels based on SELRs, since FRET is critically influenced by the distance between the fluorophores.

Calculation of FRET efficiency in a SELR-FP mixture by confocal microscopy (acceptor photobleaching)

In order to calculate *E* by confocal microscopy, hydrogels were prepared in the wells of a slide optimized for this technique and allowed to gel at room temperature (approximately 23ºC, not significant differences with spectroscopy data than for 37ºC, Table S5 and Figure S7) overnight. Figure 6 shows the images of a field of view (FOV) within the hydrogel before (Pre) and after (Post) performing photobleaching of the acceptor at its maximum λ_{ex}. As it can be seen, the intensity of the pixels for the green channel (corresponding to SELR-AcEGFP) inside the photobleached ROI increases after achieving a 93.8 ± 0.3% reduction of the intensity in the red channel (SELR-eqFP650). This is more clearly observed in the FRET (Post – Pre) picture obtained by subtraction of the Post picture from the Pre one.

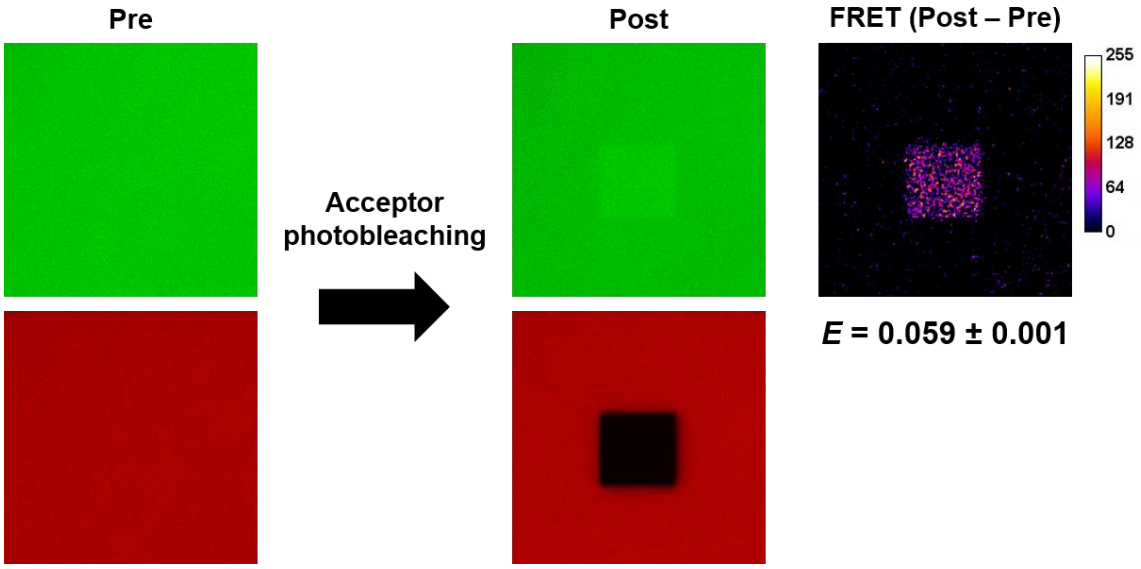

Figure 6. Diagram showing the results of SELR-AcEGFP de-quenching by photobleaching of SELR-eqFP650 through confocal microscopy. The calculated efficiency by this method was performed using Equation 4 (see Materials and Methods), and it was found to be 0.059 ± 0.01 (mean ± SD, n = 3). However, the picture showing the subtraction of the pre image from the post one does not represent exactly that efficiency, since images are not corrected.

However, the direct calculation of *E* by the Post – Pre subtraction leads to an underestimation due to partial bleaching of the whole FOV during image acquisition. For this reason, we proposed the correction of the mean intensity of the pixels inside the ROI by using another ROI close to the former, but not including that area. Then, a ratio was performed as stated in Equation 4. By this method, it was calculated $E = 0.059 \pm 0.001$ (mean ± SD, n = 3), which is lower than the efficiencies found for other FPs by microscopy methods.[30] Nevertheless, it must be taken into account the large distance between the donor λ_{em} and the acceptor λ_{ex}, which might give different advantages like avoiding bleed through or overcoming limitations derived from live fluorescence imaging due to tissue auto-fluorescence.

The discrepancy between the *E* value obtained by spectroscopy and the one calculated by acceptor photobleaching is difficult to explain and could be related to the methods used for its determination. For the calculation of FRET by spectroscopy, we relied on Equation 2, which is obtained from the simplification of more complex formulas. With this simplification, it is assumed that the excitation light intensity absorbed by the donor (SELR-AcEGFP) and all the measurement parameters are identical for both samples (donor in the absence and in the presence of acceptor, i.e. SELR-eqFP650).[31] Since both measurements were obtained simultaneously, all the settings were similar. However, the first assumption could not be confirmed due to spectral overlap between the absorption spectra of SELR-AcEGFP and the one of SELR-eqFP650 in the mixture. Hence, we relied on precise sample preparation and duplicates to avoid artifacts, which may not be completely eradicated. As regards confocal microscopy, a 100% of acceptor photobleaching was not achieved, and thereby the *E* found by this technique might not be as high as it actually is. These results can serve as an example for future works

concerning FRET, in which extraordinary care must be taken in choosing the methods used for the determination of the FRET efficiency.

Conclusions

We have developed two fluorescent SELRs able to form injectable hydrogels through the genetic fusion of two different fluorescent proteins: AcEGFP and eqFP650. Physicochemical characterization reported a thermosensitive behavior and hydrogels showed tunable mechanical properties, depending on SELR-FP concentration, hence being suitable for different applications. Furthermore, solutions and hydrogels based on these SELR-FPs showed fluorescence emission similar to the FPs on their own, except for some differences in eqFP650 excitation and emission maximum and global spectra, probably due to uncompleted maturation and/or dimerization. However, the finding of a green-shifted peak in the absorption spectrum of SELR-eqFP650, not described in the literature for the specific FP, led us to determine the FRET effect between both SELR-FPs. We calculated *E* by different methods giving dissimilar results possibly because of artifacts derived from the techniques. Furthermore, *E* values were similar for the conditions tested, hence being independent of the concentration (over a specific mid one) and of the temperature (above or below the T_t).

To our knowledge, this is the first work describing FRET between AcEGFP, or any of its derivatives, and eqFP650. Hence, we propose this system as a good model to study the FRET efficiency of novel FRET pairs. In addition, several applications may arise from this work, such as the study of self-assembled ELR-based structures (e.g. particles) and the development of hydrogels with improved traceability for tissue engineering. Similarly, SELR-FPs may find their use as biosensors, either by themselves or as

FRET-pairs, thanks to the feasible addition of binding domains, e.g. to metals or cell structures, due to their recombinant nature.

Materials and Methods

SELR-FPs design and bioproduction

In order to achieve a green emitting SELR, the AcEGFP (GenScript) was cloned and fused to the SELR. For the development of a near-infrared emitting SELR, eqFP650 gene was synthesized (NZYTech) and genetically fused to the gene encoding the recombinamer.

Cloning and heterologous expression of the SELRs used in this work were performed as described elsewhere.[32] Briefly, their full-length DNA sequences, including FPs, were obtained by the iterative recursive method through several cloning steps in XL-1 Blue Competent Cells (Agilent) and cloned into a pET-25b(+) vector to be expressed in *Escherichia coli* (BLR strain). SELRs were biosynthesized in a 15-L bioreactor (Applikon Biotechnology) and purified by several cooling and heating purification cycles (Inverse Transition Cycling) taking advantage of the ability of these recombinamers to aggregate above their transition temperature. Further centrifugation steps led to a pure product, which was dialyzed against ultra-pure water, filtered through 0.22 μm filters (Nalgene) to obtain a sterile solution, and freeze-dried prior to storage.

Physicochemical characterization of pure SELR-FPs

Characterization techniques included sodium dodecyl sulfate polyacrylamide gel electrophoresis (SDS-PAGE) and matrix-assisted laser desorption/ionization time-of-flight (MALDI-TOF) for purity and molecular weight (*Mw*) evaluation compared to the theoretical values of 128,737 Da for SELR-AcEGFP and 128,048 Da for SELR-

eqFP650; differential scanning calorimetry (DSC) to determine the T_t, i.e. the thermosensitivity of the recombinamers; HPLC to determine the amino acid composition of both SELRs after acid hydrolysis, and nuclear magnetic resonance (NMR) to provide recombinamer fingerprint data.

Rheology of SELR-FP-based hydrogels

The mechanical properties of the hydrogels formed by the SELRs above the T_t were assessed by rheological tests in a controlled stress rheometer (AR2000ex, TA Instruments) equipped with a Peltier plate for the control of the temperature and a 12 mm plate diameter for the shear stress. The procedure followed for the mechanical study was previously described.[15] SELRs were dissolved separately at 4ºC for 24 h in PBS at different concentrations, namely 1.13, 1.73 and 1.94 mM (145, 222 and 250 mg/mL, respectively). Hydrogels were formed *in situ* by depositing 200 μL of the solution on the Peltier plate (12 mm diameter) below the T_t (5ºC), and rapidly increasing the temperature to 37ºC. Time sweep experiments were run at a constant strain of 0.5% and a frequency of 1 Hz. Furthermore, the mechanical properties of a 1:1 molar mixture of both SELRs at the same concentrations were also evaluated following the same protocol.

Fluorescence spectroscopy of SELR-FPs

A multi-mode microplate reader (SpectraMax M2e, Molecular Devices) was used for the characterization of the two SELR-FPs in terms of absorption and fluorescence emission. Molar extinction coefficients (ε) were calculated using Lambert-Beer's law and the absorbance (A) of a solution of each SELR-FP at their maximum at a concentration (C) of 10 mg/mL in PBS, in a 1-cm light path (l) cuvette, at 37ºC

(Equation 1). A solution of SELR without FPs was used as reference at the same concentration.

$$(1)\ A = \varepsilon \cdot l \cdot C$$

In the case of the absorption spectra, SELR-FPs were dissolved in ultra-pure water instead of PBS (same concentration), since all the experiments that did not require comparison with the specific FPs alone were carried out in this solvent.

Emission spectrum was obtained for each SELR-FP setting the excitation wavelength at the maximum of absorption with 50 μL of a solution prepared as described above, in black half-area 96-well plates (Corning). Excitation spectra were acquired with the experimental emission λ_{max} obtained from the previous experiment: 510 nm for SELR-AcEGFP, and 636 nm for SELR-eqFP650. A 1-nm step was used in every case. All the measurements were performed at 37ºC.

Quantum yields (QY) were obtained by comparison of the emission spectra of the SELR-FPs (475 nm and 587 nm excitation for AcEGFP and eqFP650, respectively) with those of the FPs by themselves, using the free software a|e - UV-Vis-IR Spectral Software 2.2 (FluorTools, www.fluortools.com). AcGFP1 (QY = 0.82, supplier data) was obtained from Clontech, while eqFP650 (QY = 0.24)[18] was purchased from Evrogen as TurboFP650 (commercial name). The brightness of each SELR-FP was calculated by the product of the ε and the QY and expressed relative to AcGFP1.

FRET efficiency calculation through spectroscopy (donor quenching)

Data for the calculation of FRET efficiency were collected with three different types of samples: donor only (SELR-AcEGFP) at the same molar concentration than in the mixture, acceptor only (SELR-eqFP650) at the same molar concentration than in the

mixture, and a 1:1 molar mixture of both components. SELRs were prepared at different concentrations, namely 10, 50, 100 and 200 mg/mL, in cold ultra-pure water. In order to avoid biases related to the properties of the recombinamer by itself, SELR-FPs were diluted in a solution of SELR at the same concentration. Emission spectra were obtained with the multi-mode microplate reader (SpectraMax M2e, Molecular Devices) mentioned above. Single measurements at 475/510 ($\lambda_{ex}/\lambda_{em}$) were also performed on every sample below (15ºC) and above (37ºC) the T_t.

FRET efficiency (E) was calculated by the following equation (Equation 2):[20]

$$(2)\ E = 1 - \frac{F_{DA}}{F_D}$$

where F_{DA} and F_D are the fluorescence intensities of the donor at its λ_{max} of excitation and emission (475/510 nm), in the presence and in the absence of the acceptor, respectively. Due to the emission of fluorescence by the acceptor at those λ_{max} settings, data were corrected prior to application of Equation 2 by subtracting the emission spectrum of the acceptor only sample to that of the 1:1 molar mixture.

FRET efficiency calculation through confocal microscopy (acceptor photobleaching)

In order to evaluate further the FRET efficiency, confocal microscopy was performed on hydrogels based on a 1:1 molar mixture of both SELR-FPs. For that purpose, recombinamers were dissolved at 200 mg/mL in cold ultra-pure water overnight at 4ºC. Hydrogels were formed by depositing 250 μL of the cold SELR-FPs mixture on different wells of a μ-Slide 8 Well Glass Bottom (ibidi) to allow confocal microscopy visualization through the bottom with a coverslip-like thickness.

Confocal images were obtained at 25ºC (above the T_t) with a Leica TCS SP5 confocal microscope controlled by the LAS software. Regarding donor fluorescence, an Argon laser was used for excitation, and emission was collected at 499-559 nm. On the other hand, a white laser couple to a monochromator was used for excitation of the acceptor at 587 nm, and emission was collected at 595-700 nm.

With the aim of calculating FRET efficiency through acceptor photobleaching (AB), a region of interest (ROI) was drawn on the chosen field and the following pictures were taken sequentially: 1) Pre-bleaching donor excitation and emission; 2) Pre-bleaching acceptor excitation and emission; 3) Post-bleaching donor excitation and emission; 4) Post-bleaching acceptor excitation and emission. AB was accomplished setting the white laser at λ_{ex} = 600 and 90% intensity, performing 100 laser scans inside the ROI (approximately 5 minutes of bleaching time). Calculated AB was 93.8 ± 0.3% for the SELR-eqFP650, in every case.

To calculate FRET efficiency, mean intensities of the ROI in the pre- and the post-bleaching pictures of the donor were used in the following equation (Equation 3):[33]

$$(3)\ E = 1 - \frac{I_{pre}}{I_{post}}$$

However, because of the unwanted bleaching of both donor and acceptor outside the ROI, mean intensities were corrected using the mean intensity of another ROI that did not include the photobleached area. Hence, I_{pre} and I_{post} were a result of the relation of the mean intensity in the photobleached (I_p) and in the non-photobleached (I_{np}) ROIs, therefore giving the following equation (Equation 4):

$$(4)\ E = 1 - \frac{\left(\frac{I_p}{I_{np}}\right)_{pre}}{\left(\frac{I_p}{I_{np}}\right)_{post}}$$

Acknowledgments

The authors are grateful for the funding from the European Commission (NMP-2014-646075, HEALTH-F4-2011-278557, PITN-GA-2012-317306 and MSCA-ITN-2014-642687), MINECO of the Spanish Government (MAT2016-78903-R, MAT2016-79435-R, MAT2013-42473-R, MAT2013-41723-R and MAT2012-38043), Junta de Castilla y León (VA244U13 and VA313U14) and Centro en Red de Medicina Regenerativa y Terapia Celular de Castilla y León. We also want to thank Cristina Sánchez Vicente for her help in acquiring and processing confocal images.

Supporting Information

Supporting information is available free of charge on the ACS Publications Website. Schematic representation of SELR-FPs, physicochemical characterization data regarding SELR-FPs, comparison of the mechanical properties with SELR only and absorbance spectra of both SELR-FPs.

Conflicts of interest

The authors declare no competing financial interest.

List of abbreviations

ELR: elastin-like recombinamer

SELR: silk-elastin-like recombinamer

FP: fluorescent protein

AcEGFP: *Aequorea coerulescens* enhanced green fluorescent protein

FRET: Förster resonance energy transfer

Val: valine

Pro: proline

Gly: glycine

T_t: transition temperature

Mw: molecular weight

DSC: differential scanning calorimetry

ε: extinction coefficient

A: absorbance

QY: quantum yield

E: FRET efficiency

λ_{max}: wavelength at excitation/emission maximum

λ_{ex}: excitation wavelength

λ_{em}: emission wavelength

FOV: field of view

ROI: region of interest

F_{DA}: fluorescence intensity of donor at its λ_{max} of excitation in the presence of the acceptor

F_D: fluorescence intensity of donor at its λ_{max} of excitation in the absence of the acceptor

AB: acceptor photobleaching

I_{pre}: fluorescence intensity before acceptor photobleaching

I_{post}: fluorescence intensity after acceptor photobleaching

I_p: fluorescence intensity in a photobleached ROI

I_p: fluorescence intensity in a non-photobleached ROI

References

(1) Ahadian, S., Sadeghian, R. B., Salehi, S., Ostrovidov, S., Bae, H., Ramalingam, M., and Khademhosseini, A. (2015) Bioconjugated Hydrogels for Tissue Engineering and Regenerative Medicine. *Bioconjugate Chemistry 26*, 1984-2001.

(2) Girotti, A., Orbanic, D., Ibáñez-Fonseca, A., Gonzalez-Obeso, C., and Rodríguez-Cabello, J. C. (2015) Recombinant Technology in the Development of Materials and Systems for Soft-Tissue Repair. *Advanced Healthcare Materials 4*, 2423-2455.

(3) Urry, D. W., Cunningham, W. D., and Ohnishi, T. (1974) Studies on the conformation and interactions of elastin. Proton magnetic resonance of the repeating pentapeptide. *Biochemistry 13*, 609-16.

(4) Yeo, G. C., Aghaei-Ghareh-Bolagh, B., Brackenreg, E. P., Hiob, M. A., Lee, P., and Weiss, A. S. (2015) Fabricated Elastin. *Advanced Healthcare Materials 4*, 2530-2556.

(5) Kowalczyk, T., Hnatuszko-Konka, K., Gerszberg, A., and Kononowicz, A. K. (2014) Elastin-like polypeptides as a promising family of genetically-engineered protein based polymers. *World Journal of Microbiology and Biotechnology 30*, 2141-2152.

(6) Arias, F. J., Mercedes, S., Alicia, F.-C., Guillermo, P., and Alessandra, G. (2014) Recent Contributions of Elastin-Like Recombinamers to Biomedicine and Nanotechnology. *Current Topics in Medicinal Chemistry 14*, 819-836.

(7) Urry, D. W. (1993) Molecular Machines: How Motion and Other Functions of Living Organisms Can Result from Reversible Chemical Changes. *Angewandte Chemie International Edition in English 32*, 819-841.

(8) Ribeiro, A., Arias, F. J., Reguera, J., Alonso, M., and Rodríguez-Cabello, J. C. (2009) Influence of the Amino-Acid Sequence on the Inverse Temperature Transition of Elastin-Like Polymers. *Biophysical Journal 97*, 312-320.

(9) McDaniel, J. R., Radford, D. C., and Chilkoti, A. (2013) A Unified Model for De Novo Design of Elastin-like Polypeptides with Tunable Inverse Transition Temperatures. *Biomacromolecules 14*, 2866-2872.

(10) Herrero-Vanrell, R., Rincón, A. C., Alonso, M., Reboto, V., Molina-Martinez, I. T., and Rodríguez-Cabello, J. C. (2005) Self-assembled particles of an elastin-like polymer as vehicles for controlled drug release. *Journal of Controlled Release 102*, 113-122.

(11) Martín, L., Castro, E., Ribeiro, A., Alonso, M., and Rodríguez-Cabello, J. C. (2012) Temperature-Triggered Self-Assembly of Elastin-Like Block Co-Recombinamers:The Controlled Formation of Micelles and Vesicles in an Aqueous Medium. *Biomacromolecules 13*, 293-298.

(12) Putzu, M., Causa, F., Nele, V., Torre, I. G. d., Rodriguez-Cabello, J. C., and Netti, P. A. (2016) Elastin-like-recombinamers multilayered nanofibrous scaffolds for cardiovascular applications. *Biofabrication 8*, 045009.

(13) Martín, L., Alonso, M., Girotti, A., Arias, F. J., and Rodríguez-Cabello, J. C. (2009) Synthesis and Characterization of Macroporous Thermosensitive Hydrogels from Recombinant Elastin-Like Polymers. *Biomacromolecules 10*, 3015-3022.

(14) Cappello, J., Crissman, J., Dorman, M., Mikolajczak, M., Textor, G., Marquet, M., and Ferrari, F. (1990) Genetic Engineering of Structural Protein Polymers. *Biotechnology Progress 6*, 198-202.

(15) Fernández-Colino, A., Arias, F. J., Alonso, M., and Rodríguez-Cabello, J. C. (2014) Self-Organized ECM-Mimetic Model Based on an Amphiphilic Multiblock Silk-Elastin-Like Corecombinamer with a Concomitant Dual Physical Gelation Process. *Biomacromolecules 15*, 3781-3793.

(16) Gurskaya, N. G., Fradkov, A. F., Pounkova, N. I., Staroverov, D. B., Bulina, M. E., Yanushevich, Y. G., Labas, Y. A., Lukyanov, S., and Lukyanov, K. A. (2003) A colourless green fluorescent protein homologue from the non-fluorescent hydromedusa Aequorea coerulescens and its fluorescent mutants. *Biochemical Journal 373*, 403-408.

(17) Cormack, B. P., Valdivia, R. H., and Falkow, S. (1996) FACS-optimized mutants of the green fluorescent protein (GFP). *Gene 173*, 33-38.

(18) Shcherbo, D., Shemiakina, I. I., Ryabova, A. V., Luker, K. E., Schmidt, B. T., Souslova, E. A., Gorodnicheva, T. V., Strukova, L., Shidlovskiy, K. M., Britanova, O. V., *et al.* (2010) Near-infrared fluorescent proteins. *Nat Meth 7*, 827-829.

(19) Kobayashi, H., Ogawa, M., Alford, R., Choyke, P. L., and Urano, Y. (2010) New Strategies for Fluorescent Probe Design in Medical Diagnostic Imaging. *Chemical Reviews 110*, 2620-2640.

(20) Lakowicz, J. R. (2006) *Principles of Fluorescence Spectroscopy*, 3 ed., Springer US.

(21) Day, R. N., and Davidson, M. W. (2012) Fluorescent proteins for FRET microscopy: Monitoring protein interactions in living cells. *BioEssays 34*, 341-350.

(22) Fujita, Y., Funabashi, H., Mie, M., and Kobatake, E. (2007) Design of a Thermocontrollable Protein Complex. *Bioconjugate Chemistry 18*, 1619-1624.

(23) Obeng, E. M., Dullah, E. C., Danquah, M. K., Budiman, C., and Ongkudon, C. M. (2016) FRET spectroscopy-towards effective biomolecular probing. *Analytical Methods 8*, 5323-5337.

(24) Hsieh, H. V., Sherman, D. B., Andaluz, S. A., Amiss, T. J., and Pitner, J. B. (2012) Fluorescence Resonance Energy Transfer Glucose Sensor from Site-Specific Dual Labeling of Glucose/Galactose Binding Protein Using Ligand Protection. *Journal of Diabetes Science and Technology 6*, 1286-1295.

(25) Voss, S., Fischer, R., Jung, G., Wiesmüller, K.-H., and Brock, R. (2007) A Fluorescence-Based Synthetic LPS Sensor. *Journal of the American Chemical Society 129*, 554-561.

(26) Hussain, S. A., Dey, D., Chakraborty, S., Saha, J., Roy, A. D., Chakraborty, S., Debnath, P., and Bhattacharjee, D. (2015) Fluorescence Resonance Energy Transfer (FRET) sensor. *Journal of Spectroscopy and Dynamics 5*.

(27) Carlson, H. J., and Campbell, R. E. (2009) Genetically encoded FRET-based biosensors for multiparameter fluorescence imaging. *Current Opinion in Biotechnology 20*, 19-27.

(28) Christensen, T., Hassouneh, W., Trabbic-Carlson, K., and Chilkoti, A. (2013) Predicting Transition Temperatures of Elastin-Like Polypeptide Fusion Proteins. *Biomacromolecules 14*, 1514-1519.

(29) Pal, S. (2014) Mechanical Properties of Biological Materials, in *Design of Artificial Human Joints & Organs* pp 23-40, Springer US, Boston, MA.

(30) Suzuki, A., Badger, B. L., Haase, J., Ohashi, T., Erickson, H. P., Salmon, E. D., and Bloom, K. (2016) How the kinetochore couples microtubule force and centromere stretch to move chromosomes. *Nat Cell Biol 18*, 382-392.

(31) Hildebrandt, N. (2013) How to Apply FRET: From Experimental Design to Data Analysis, in *FRET – Förster Resonance Energy Transfer* pp 105-163, Wiley-VCH Verlag GmbH & Co. KGaA.

(32) Rodriguez-Cabello, J. C., Girotti, A., Ribeiro, A., and Arias, F. J. (2012) Synthesis of genetically engineered protein polymers (recombinamers) as an example of advanced self-assembled smart materials. *Methods in molecular biology 811*, 17-38.

(33) Bajar, B. T., Wang, E. S., Zhang, S., Lin, M. Z., and Chu, J. (2016) A Guide to Fluorescent Protein FRET Pairs. *Sensors (Basel, Switzerland) 16*.

TOC GRAPHIC